Antiferromagnetic fluctuations and d-wave superconductivity in electron-doped high-temperature superconductors

Bumsoo Kyung[1], Jean-Sébastien Landry[1], and A.-M.S. Tremblay[1,2]
[1] *Département de physique and Regroupement québécois sur les matériaux de pointe,*
[2] *Institut canadien de recherches avancées, Université de Sherbrooke, Sherbrooke, Québec, Canada, J1K 2R1*
(Dated: February 6, 2008)

We show that, at weak to intermediate coupling, antiferromagnetic fluctuations enhance d-wave pairing correlations until, as one moves closer to half-filling, the antiferromagnetically-induced pseudogap begins to suppress the tendency to superconductivity. The accuracy of our approach is gauged by detailed comparisons with Quantum Monte Carlo simulations. The negative pressure dependence of T_c and the existence of photoemission hot spots in electron-doped cuprate superconductors find their natural explanation within this approach.

For almost two decades, the mechanism for high temperature superconductivity has been one of the main issues in condensed matter physics. Despite an extensive body of theoretical work, there is at present no consensus about the mechanism. This is mainly due to lack of a reliable theoretical tool for a strong coupling problem where the value of the on-site Coulomb interaction U is of the order of, or larger than, the bandwidth [1]. The situation, however, appears more promising for electron-doped high-temperature superconductors (e-HTSC) in which the charge gap at half-filling is 25% smaller than that of hole-doped cuprates (h-HTSC), suggesting a smaller value of U [2]. This offers an opportunity for theories of d-wave superconductivity based on weak- to intermediate-coupling approaches [3, 4, 5].

In this communication, we show that improved theoretical calculations can indeed describe several aspects of e-HTSC that were unexplained by previous calculations. For example, we show that the negative pressure derivative of the superconducting transition temperature T_c of e-HTSC, which contrasts with the positive pressure derivative of h-HTSC, can be explained. In addition, the hot spots observed in Angle Resolved Photoemission Experiments (ARPES) also come out of the calculation. We also discuss how a decrease in T_c in the underdoped region can occur when a large pseudogap is produced by antiferromagnetic (AFM) fluctuations. Previous calculations [6] predicted that T_c would increase monotonically as one approaches half-filling.

Let us first consider the results of numerical calculations concerning the possibility of d-wave superconductivity in the Hubbard model. In Fig.1 we present a rather detailed survey of the $d_{x^2-y^2}$-wave susceptibility χ_d obtained from Quantum Monte Carlo (QMC) calculations [7, 8, 9, 10] for the Hubbard model. The Hubbard model is characterized, as usual, by nearest-neighbor hopping t and on-site repulsion U. By contrast with variational methods, the QMC calculations are unbiased. They also can be performed on much larger lattices than exact diagonalizations. QMC is essentially exact, within statistical error bars that, in Fig. 1, are generally smaller than the symbol size. As usual, the $d_{x^2-y^2}$-wave susceptibility is

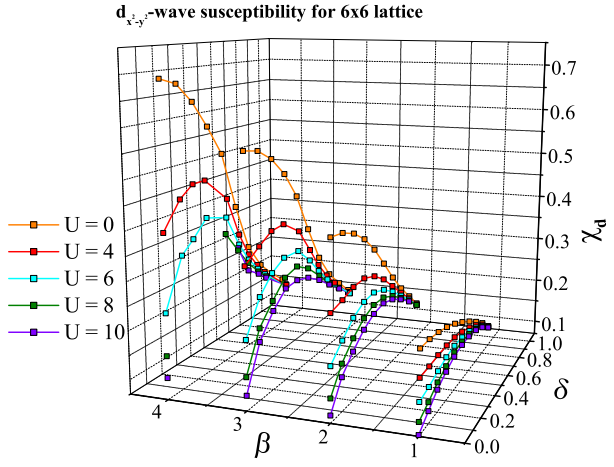

FIG. 1: (Color) The $d_{x^2-y^2}$ susceptibility obtained from QMC simulations as a function of doping and of temperature for a 6×6 lattice. Various values of U correspond to different colors. The size dependence of the results is small at these temperatures. The Trotter step size is $\Delta\tau = 1/10$ while the number of measurements at each point in parameter space is around 10^5. Measurements are grouped in blocs of 125 and stabilized every five steps along the imaginary-time axis.

defined by $\chi_d = \int_0^\beta d\tau \left\langle T_\tau \Delta(\tau) \Delta^\dagger \right\rangle$ with the d-wave order parameter $\Delta^\dagger = \sum_i \sum_\gamma g(\gamma) c^\dagger_{i\uparrow} c^\dagger_{i+\gamma\downarrow}$ the sum over γ being over nearest-neighbors, with $g(\gamma) = \pm 1/2$ depending on whether γ is a neighbor along the $\widehat{\mathbf{x}}$ or the $\widehat{\mathbf{y}}$ axis. From now on, we work in units where $k_B = 1$, $\hbar = 1$, lattice spacing and hopping t are unity. The results are shown for various temperatures $T = \beta^{-1}$, dopings δ and interaction strengths U (shown by the various colors). The data clearly shows that the dome shape dependence of χ_d is present not only for strong coupling ($U \gtrsim 8$),but also at weak to intermediate coupling ($U = 4$). For weak coupling the dome shape occurs at temperatures that are sufficiently low ($\beta = 4$) for AFM (or spin-density-wave) correlations to build up. It has been known for a long time that these results, obtained by a numerical method of choice, by themselves do not suffice to decide whether

there is a d-wave superconducting phase in the Hubbard model. Indeed, the susceptibility should diverge if there is a phase transition. Also, at $\beta = 4$ the non-interacting model, $U = 0$, has a larger susceptibility than the $U \neq 0$ model, a fact that does not encourage optimism.

To conclusively verify whether d-wave superconductivity exists in this model at weak to intermediate coupling, one needs to reach temperatures that are an order of magnitude smaller than those shown in Fig.1. As is well known, the so-called sign-problem renders impossible simulations at these low temperatures. To reach such temperatures, we use the Two-Particle Self-Consistent approach [11, 12] (TPSC) and extend it to compute superconducting correlations. The accuracy of the method for spin fluctuations and self-energy has already been proven [11, 13] by comparisons with QMC data. In particular, there is a pseudogap of AFM origin at a crossover temperature T_X.

Briefly speaking, to extend TPSC to compute pairing susceptibility, we begin from the Schwinger-Martin-Kadanoff-Baym formalism with both diagonal [11, 12] and off-diagonal [14] source fields. The self-energy is expressed in terms of spin and charge fluctuations and the irreducible vertex entering the Bethe-Salpeter equation for the pairing susceptibility is obtained from functional differentiation. The final expression for the d-wave susceptibility is,

$$\chi_d\left(\mathbf{q}=0, iq_n=0\right) = \frac{T}{N}\sum_k \left(g_d^2\left(\mathbf{k}\right) G_\uparrow^{(2)}\left(-k\right) G_\downarrow^{(2)}\left(k\right)\right) - \frac{U}{4}\left(\frac{T}{N}\right)^2 \sum_{k,k'} g_d\left(\mathbf{k}\right) G_\uparrow^{(2)}\left(-k\right) G_\downarrow^{(2)}\left(k\right) \times \left(\frac{3}{1-\frac{U_{sp}}{2}\chi_0\left(k'-k\right)} + \frac{1}{1+\frac{U_{ch}}{2}\chi_0\left(k'-k\right)}\right) G_\uparrow^{(1)}\left(-k'\right) G_\downarrow^{(1)}\left(k'\right) g_d\left(\mathbf{k}'\right). \quad (1)$$

In the above expression, Eq.(1), $g_d\left(\mathbf{k}\right)$ is the form factor for the gap symmetry, while k and k' stand for both wavevector and Matsubara frequencies $k \equiv \left(\mathbf{k}, \left(2n+1\right)\pi T\right)$ on a square-lattice with N sites at temperature T. The spin and charge susceptibilities take the form $\chi_{sp}^{-1}\left(q\right) = \chi_0(q)^{-1} - \frac{U_{sp}}{2}$ and $\chi_{ch}^{-1}\left(q\right) = \chi_0(q)^{-1} + \frac{U_{ch}}{2}$ with χ_0 computed with the Green function $G_\sigma^{(1)}$ that contains the self-energy whose functional differentiation gave the spin and charge vertices. The values of U_{sp}, U_{ch} and $\langle n_\uparrow n_\downarrow\rangle$ are obtained [15] from $U_{sp} = U\left\langle n_\uparrow n_\downarrow\right\rangle / \left(\left\langle n_\uparrow\right\rangle \left\langle n_\downarrow\right\rangle\right)$ and from the local-moment sum-rule. In the pseudogap regime, one cannot use $U_{sp} = U\left\langle n_\uparrow n_\downarrow\right\rangle / \left(\left\langle n_\uparrow\right\rangle \left\langle n_\downarrow\right\rangle\right)$. Instead [11], one uses the local-moment sum rule with the zero temperature value of $\langle n_\uparrow n_\downarrow\rangle$ obtained by the method of Ref. [16] that agrees very well with QMC calculations at all values of U. Also, $G_\sigma^{(2)}$ contains self-energy effects coming from spin and charge fluctuations, as described in previous work [12, 13].

The effective interaction in the particle-particle channel mediated by AFM fluctuations is represented by the second term of Eq.(1). It becomes sizeable only after spin fluctuations have become large. Eq.(1) thus contains two leading effects, namely spin and charge fluctuations influence the magnitude of the effective interactions in the particle-particle channel and they also decrease the lifetime of particles that pair (through $G_\sigma^{(2)}$). The latter effect is generally detrimental to superconductivity while the former may favor pairing.

The explicit expression for χ_d, Eq.(1), allows us to find *analytically* which gap symmetry is enhanced or suppressed by AFM fluctuations. Indeed, since near half-filling AFM fluctuations are strongly peaked at $\mathbf{k}' - \mathbf{k} = \mathbf{Q}$ (commensurate or incommensurate), the sign of $f \equiv -g_d\left(\mathbf{k}+\mathbf{Q}\right)/g_d\left(\mathbf{k}\right)$ and the magnitude of $g_d\left(\mathbf{k}\right)$ near the Fermi wave vector $\mathbf{k}_F$ determine the most favorable gap symmetry. Within a spin-singlet subspace, s-wave and d_{xy}-wave symmetries are suppressed since $f < 0$. Extended s-wave symmetry has $f > 0$, just like $d_{x^2-y^2}$-wave, but its form factor is much smaller near $\mathbf{k}_F$, so we take $g_d\left(k\right) = \left(\cos k_x - \cos k_y\right)$.

Let us first verify the accuracy of this approach by comparing, in Fig.2, the QMC results for χ_d, shown by symbols, with those of the generalized TPSC approach, Eq.(1), indicated by the solid line. The case $U = 0$, $\beta = 4$ is for reference. Fig. 2 demonstrates that the approach, Eq.(1), agrees very well with QMC results for χ_d at $U = 4$. The agreement improves for lower values of U. When the interaction strength reaches the intermediate coupling regime, $U = 6$, deviations of the order of 20 to 30% may occur but the qualitative dependence on temperature and doping remains accurate. The inset shows that previous spin-fluctuation calculations (FLEX) in two dimensions [3, 6] deviate both qualitatively and quantitatively from the QMC results. More specifically, in the FLEX approach χ_d does not show a pronounced maximum at finite doping. Moreover, it is known from previous work that FLEX does not show a pseudogap in the single-particle spectral weight at the Fermi surface [13]. In TPSC the pseudogap is the key ingredient that

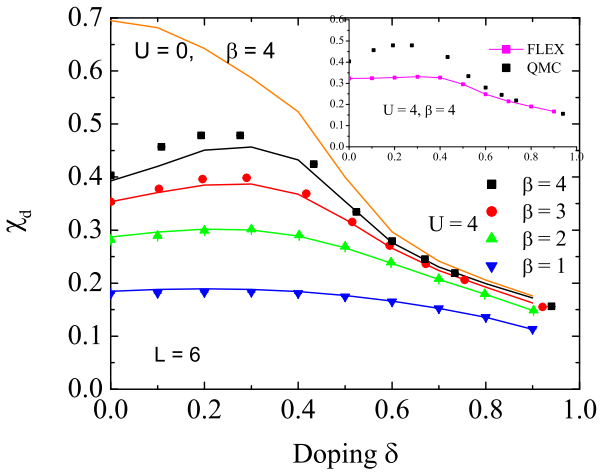

FIG. 2: (Color online) Comparisons between the $d_{x^2-y^2}$ susceptibility obtained from QMC simulations (see previous figure) and from the approach described in the present work. QMC error bars are smaller than the symbols. Analytical results are joined by solid lines. Both calculations are for $U = 4$, a 6×6 lattice and four different temperatures. The case $U = 0, \beta = 4$ is shown for reference. The size dependence of the results is small at these temperatures. The inset compares QMC and FLEX at $U = 4, \beta = 4$.

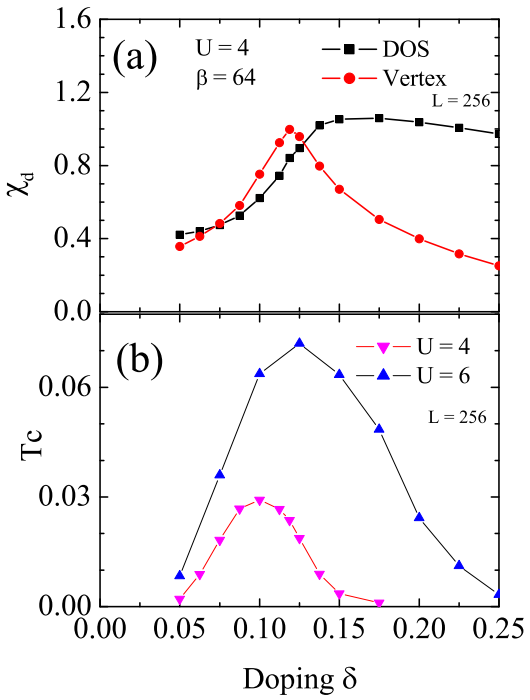

FIG. 3: (Color online) Part (a) shows the contributions from the first term (DOS) and second term (vertex) of Eq.(1). In (b), our estimate of T_c using the Thouless criterion for $U = 4$ and $U = 6$.

leads to a decrease in T_c in the underdoped regime.

In TPSC we can understand why, as mentioned above, χ_d is smaller than the non-interacting value in this temperature range. Indeed, the main contribution is from the first term in Eq.(1) which represents a pair of propagating particles that do not interact with each other. The contribution of the second term, which represents interaction through the exchange of spin and charge fluctuations, is, for $\beta = 4$, about 1% at $\delta = 0.5$, growing to only 22% at $\delta = 0$. Hence, in this temperature range, χ_d is smaller than the non-interacting value because of the decrease in spectral weight at $\omega = 0$ brought about by AFM self-energy effects.

While it is impossible to do QMC calculations at lower T, the analytical formula for χ_d, Eq.(1), can be extended to low T and to 256×256 lattice size using renormalization group acceleration [17] and Fast Fourier Transforms. This allows us to verify whether there is d-wave superconductivity ($d - SC$) in the Hubbard model at weak to intermediate coupling. The complete Bethe-Salpeter equation would contain the possibility of repeatedly exchanging spin fluctuations. Eq.(1) contains only the first two terms, namely the zero and the one spin- and charge fluctuation exchange. As for the expansion $(1-x)^{-1} \sim 1+x$, the divergence should occur when the first two terms have the same magnitude. We can thus estimate T_c for $d - SC$. As usual, the T_c obtained from the divergence of the infinite series (Thouless criterion) should give an upper bound to the Kosterlitz-Thouless transition temperature T_{KT} expected in $d = 2$. In Fig.3 (a) the first (DOS) and second (Vertex) contributions in Eq.(1) are plotted for $U = 4$ at $\beta = 64$ as a function of doping. The vertex part becomes larger than the first part over a range of δ. This signals, according to our criterion, that $0.07 < \delta < 0.13$ is below T_c at $\beta = 64$. Note that it is because the vertex part decreases much faster than the DOS part near half-filling that the $d-SC$ stops close to half-filling, leading to a dome shape in T_c. The fast decrease of the vertex part near half-filling is because it has its strongest contribution near the Fermi surface where the pseudogap effect is most pronounced.

The solid lines with symbols in Fig. 3(b) give the value of T_c estimated for two values of U in the intermediate coupling regime. The $U = 6$ results should be viewed as giving the qualitative trend with increasing U. As is clear by now, the decrease of T_c near half-filling is caused by the same AFM fluctuations that enhance $d - SC$ at large doping. $d - SC$ fluctuations in our approach are important only between T_c and T_{KT}, by contrast with phase fluctuation theories at strong coupling [18]. Our results also contrast with theories where the decrease of T_c is driven by hidden competing broken symmetry [19].

To make more detailed connection with experimental results on e-HTSC, one should add second-neighbor t' and third-neighbor t'' hopping to the Hamiltonian, as suggested by band-structure calculations and by ARPES. We perform the usual particle-hole transformation that

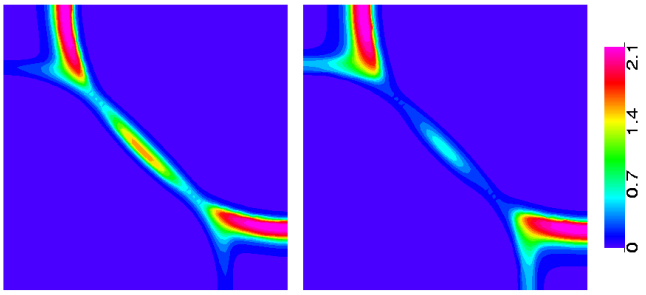

FIG. 4: (Color) Fermi surface plots obtained from energy dispersion curves integrated from -0.2 to 0.1 with $|t'| = 0.175$, $|t''| = 0.05$. On both plots, $\delta = 0.15$, $\beta = 40$, system size 128×128. In (a), $U = 5.75$ (b) $U = 6.25$.

maps electron-doping of the negative t' model to hole doping with positive t'. As t' and t'' increase, AFM fluctuations are frustrated, so pseudogap effects become less important and the fall of T_c on the underdoped side becomes less and less pronounced. Including AFM coupling in the third dimension would lead to a real AFM transition that would eventually overcome the pairing instability. The more significant result we want to draw attention to is that, assuming that applying pressure only increases t (and thus decreases U/t), the data of Fig. 3 shows that $d \ln T_c/dP < 0$ in the weak to intermediate coupling regime described by our approach. This remains true with finite t' and t'' and agrees with the experimental negative pressure dependence of T_c in these compounds [20]. By contrast, in h-HTSC $d \ln T_c/dP$ has the opposite sign. If antiferromagnetism plays a role in the superconductivity of both e-HTSC and h-HTSC, then the positive sign of $d \ln T_c/dP$ in the latter may be understood from the fact that they are in the strong-coupling regime where $J = 4t^2/U$ increases with pressure.

Fig. 4 shows Fermi surface maps for all wave vectors $\mathbf{k}$ in the first quadrant of the Brillouin zone. The maps are obtained, as in ARPES experiments on NCCO [21], from the integral of the single-particle spectral weight $A(\mathbf{k}, \omega)$ times the Fermi function over a frequency range running from -0.2 to $+0.1$. For $U = 5.75$, shown on the left-hand side, two hot spots are clearly apparent at the intersection of the Fermi surface with the AFM zone boundary, as observed experimentally at optimal doping. The AFM correlation length ξ is 12 lattice spacings for this plot and the spin susceptibility at (π, π) is much larger than the non-interacting value. At this β and for this value of U, a pseudogap is observed only at the hot spots. They appear because the strong low-energy AFM fluctuations can scatter excitations at these points to other points on the Fermi surface separated by (π, π) [22]. If U is not large enough, there is only a decrease of spectral weight at the hot spots instead of a real pseudogap. By contrast, the right-hand side of Fig. 4 shows that if the interaction is too large, $U = 6.25$ ($\xi = 18$), the AFM fluctuations scatter so strongly that a pseudogap appears everywhere along an arc on the Fermi surface. This confirms our contention that U cannot be too large near optimal doping in e-HTSC to explain the experimental results. The value of U, however, does have to increase with decreasing δ so as to recover the Fermi maps observed at $\delta = 10\%$ as well as the Mott insulator at half-filling [23, 24].

In summary, in e-HTSC the symmetry of the superconducting order parameter, the dependence of T_c on pressure, as well as the hot spots observed by ARPES at optimal doping can all be explained by the Hubbard model at weak to intermediate coupling. Generally, antiferromagnetic fluctuations help superconductivity until they are so strong that they open up a pseudogap that hinders $d - SC$.

We are especially grateful to V. Hankevych for discussions and for performing some of the calculations. We also thank S. Allen, C. Bourbonnais, A.-M. Daré, P. Fournier and D. Sénéchal for useful discussions. This work was partially supported by the Natural Sciences and Engineering Research Council of Canada (NSERC), by the Fonds pour la Formation de Chercheurs et l'Aide à la Recherche (FCAR) from the Québec government, by the Canadian Institute for Advanced Research and by the Tier I Canada Research Chair program (A.-M.S.T).

[1] R. Coldea *et al.* Phys. Rev. Lett. **86**, 5377 (2001).
[2] S. Uchida *et al.* Physica C, 162, 1677 (1989).
[3] N.E. Bickers *et al.,* Phys. Rev. Lett. **62**, 961 (1989).
[4] Andrey V. Chubukov *et al.,* cond-mat/0201140.
[5] J. P. Carbotte *et al.* Nature (London), 401, 354 (1999).
[6] C.-H. Pao , *et al.* Phys. Rev. B **51**, 16 310 (1995).
[7] J.E. Hirsch and H.Q. Lin, Phys. Rev. B **37**, 5070 (1988).
[8] S.R. White *et al.,* Phys. Rev. B **39**, 839 (1989).
[9] A. Moreo *et al.,* Phys. Rev. B **43**, 8211 (1991).
[10] R.T. Scalettar *et al.,* Phys. Rev. Lett. **67**, 370 (1991).
[11] Y.M. Vilk *et al.,* J. Phys. I (France) **7**, 1309 (1997).
[12] S. Allen, *et al.* in *"Theoretical Methods for Strongly Correlated Electrons", (Springer, New York, 2003)* D. Sénéchal, *et al.* (eds.)
[13] S. Moukouri *et al.,* Phys. Rev. B **61**, 7887 (2000).
[14] S. Allen *et al.,* Phys.Rev. B **64**, 075115 (2001).
[15] Y.M. Vilk *et al.,* Phys. Rev. B **49**, 13 267 (1994).
[16] L. Lilly *et al.,* Phys. Rev. Lett. **65,** 1379 (1990).
[17] C.-H. Pao *et al.,* Phys. Rev. B **49**, 1586 (1994).
[18] V. J. Emery *et al.*, Nature, London **374**, 434 (1995).
[19] S. Chakravarty *et al.*, Phys. Rev. B **63**, 094503 (2001).
[20] M.B. Maple, MRS Bulletin, June, 60 (1990).
[21] N. P. Armitage *et al.,* Phys. Rev. Lett. **87**, 147003 (2001).
[22] G. Preosti *et al.* Phys. Rev. B **59**, 1474 (1999).
[23] C. Kusko, *et al.* Phys. Rev. B **66**, 140513 (2002); R. S. Markiewicz (unpublished).
[24] D. Sénéchal *et al.* (unpublished).